International Journal of Heat and Mass Transfer 258 (2026) 128311

Contents lists available at ScienceDirect

International Journal of Heat and Mass Transfer

journal homepage: www.elsevier.com/locate/hmt

Convective mass transfer boundary conditions

S.B. Beale *

Institute of Energy Technologies, IET-3, Forschungszentrum Jülich, Jülich, 52425, Germany
Mechanical and Materials Engineering, Queen's University, Kingston, K7L 3N6, Ontario, Canada

ARTICLE INFO

Keywords:
Numerical heat and mass transfer
Boundary conditions
Finite volume method
Computational fluid dynamics
Modeling

ABSTRACT

The prescription for convective mass transfer boundary conditions is derived in a linearized form as a function of the mass fraction, with the mixture convection flux and the transferred substance-state as the coefficient and value, respectively. It is shown that all the basic boundary conditions of computational fluid dynamics; inlet, outlet, wall, etc. may be essentially seen as specific instances derived from this simple prototype. Details of how to calculate boundary values and gradients from the driving force are provided. In addition to being applicable to mass transfer problems, where the dependent variable is mass fraction or concentration; the theory is also relevant to heat and momentum transfer for fluid flow problems with injection/suction along the boundaries. The key concepts of the convective mass transfer boundary condition are derived for a basic finite-volume cell, with a critical discussion of the magnitude of the errors that are introduced when simplified formulations are employed at the boundaries. This study bridges and extends traditional mass transfer theory and best practices in computational fluid dynamics.

1. Introduction

The finite volume method has enjoyed widespread use for several decades; together with related methods such as finite difference and finite element methods, it forms a cornerstone in computational fluid dynamics (CFD) and numerical heat and mass transfer. The formulation of boundary conditions (BCs) is an important subject in CFD/numerical heat and mass transfer; one that has not received much attention in comparison to others, such as meshing and model closures, although in the past symposium and journal special editions [1] have occasionally been devoted to the subject. The importance of BCs in CFD and numerical heat and mass transfer is not to be understated; BCs are frequently simplified, and as a result not only introduce numerical errors into the final solution, but ultimately can actually change the nature of the problem. BCs represent idealizations of reality, necessary to obtain a reasonable numerical solution for the particular problem under consideration. Constant values of velocity, pressure, and temperature (Dirichlet conditions) or constant gradients/fluxes (Neumann conditions) are often assumed to occur in relative proximity to the domain of interest, for example at inlets, outlets, and walls. A clear and rigorous understanding of BCs is an integral part of any numerical solution procedure.

The purpose of this paper is to introduce the reader to mass transfer boundary value problems, typically encountered in mechanical and chemical engineering applications, in a form they may not have encountered before. A particular issue associated with mass transfer is the fact that neither the desired boundary value nor the flux/gradient are necessarily known, *a priori*. It is shown how these non-linear wall values may be computed, during the solution procedure. A number of different approaches have been considered in the past. For reasons explained below, the author favors formulations based on the concept of the 'transferred substance state' (T-state); a notion originally developed in the standard mass transfer formulation of Spalding [2], which was first introduced over 60 years ago in a remarkable paper published in Volume 1 of the International Journal of Heat and Mass Transfer. This formulation unified multiple branches of engineering disciplines involving mass transfer, and predates CFD. The present author has adapted these concepts for modern CFD applications. Some of the underlying concepts have been previously introduced for specific applications [3–5]; however a comprehensive discussion of the convective mass transfer boundary condition (CMTBC) problem in the context of CFD has not been published before. The emphasis here is on physical aspects of the underlying transport processes which form the basis for numerical schemes.

There are numerous practical applications for mass transfer theory in engineering science. Two particularly salient areas are: membrane separations and chemical reactors. These have been treated by a number of authors using CFD codes and methods. In membrane technology; there have been a number of review articles on the use of CFD, for example; [6–8]. Similarly mass transfer in chemical reactors has been

* Correspondence to: Institute of Energy Technologies, IET-3, Forschungszentrum Jülich, Jülich, 52425, Germany.
E-mail addresses: s.beale@fz-juelich.de, steven.beale@queensu.ca.

https://doi.org/10.1016/j.ijheatmasstransfer.2025.128311
Received 15 October 2025; Received in revised form 16 December 2025; Accepted 22 December 2025
Available online 2 January 2026

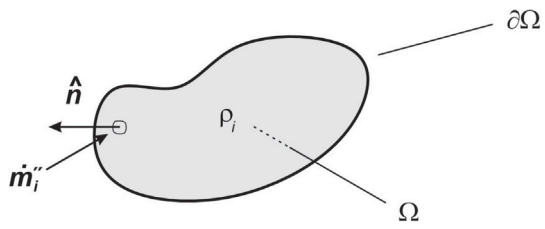

Fig. 1. Arbitrary element of volume, Ω with corresponding boundary surface $\partial\Omega$.

discussed in the books by Oran and Boris [9], Probstein [10] and elsewhere.

This present work makes the following contributions:

- The work combines basic mass transfer theory with modern CFD practices to yield a simple formulation for numerical mass transfer boundary conditions.
- The formulation is quite general and may be applied to a large set of applications, including mass/heat transfer, laminar/turbulent, phase change, reacting flow, etc.
- The validity of the present approach is illustrated by comparison to the pioneering work of Sherwood et al. with excellent agreement.
- Conventional CFD boundary conditions (inlets, outlets, walls) may be considered as specific instantiations of the CMTBC.
- Issues associated with prescribing wall mass fractions are discussed. These may often be circumvented by simply employing CMTBCs.

2. Basic equations

2.1. Species conservation

The principle of conservation of mass for species, i, in a mixture, may be expressed as follows [11–13]

$$\frac{\partial \rho_i}{\partial t} + \nabla \cdot (\rho_i \boldsymbol{U}_i) = 0 \text{ in } \Omega \tag{1}$$

where, with reference to Fig. 1, Ω is an arbitrary volumetric region bounded by surface $\partial\Omega$, and ρ_i is the partial density of species i. Eq. (1) is quite general and is considered to be true for all piecewise-smooth (i.e., differentiable) continua.

Let the mass fraction $y_i = \rho_i/\rho$ [kg/kg], where the mixture density, $\rho = \sum_{i=1}^{n} \rho_i$, and the diffusion flux vector, $\boldsymbol{j}_i''$ is given by,

$$\boldsymbol{j}_i'' = \rho_i \left(\boldsymbol{U}_i - \boldsymbol{U}\right) = \rho y_i \left(\boldsymbol{U}_i - \boldsymbol{U}\right) \tag{2}$$

where $\boldsymbol{U} = \sum_{i=1}^{n} \rho_i \boldsymbol{U}_i/\rho$ is the mixture velocity. The reader will note that the total flux of i is the sum of the convective and diffusive fluxes, $\rho_i \boldsymbol{U}_i = \rho \boldsymbol{U} y_i + \boldsymbol{j}_i''$. Defining the species mass flux by, $\dot{\boldsymbol{m}}_i'' = \rho \boldsymbol{U}_i y_i$ and the overall/mixture mass flux as, $\dot{\boldsymbol{m}}'' = \rho \boldsymbol{U} = \sum_{i=1}^{n} \dot{\boldsymbol{m}}_i''$, it follows that the diffusion flux may also be written as $\boldsymbol{j}_i'' = \dot{\boldsymbol{m}}_i'' - \dot{\boldsymbol{m}}'' y_i$.

The species equation may thus be written [14],

$$\frac{\partial}{\partial t}\left(\rho y_i\right) + \nabla \cdot \left(\rho \boldsymbol{U} y_i\right) + \nabla \cdot \boldsymbol{j}_i'' = 0 \text{ in } \Omega \tag{3}$$

There will be two or more such equations, although of the n equations, only $n-1$ are independent, since $\sum_{i=1}^{n} y_i = 1$. The nth equation is generally reserved for the overall continuity or pressure equation. For a binary or higher order (ternary etc.) mixture, where the individual species have similar molecular weights/diffusion coefficients, Fick's law may be presumed,

$$\boldsymbol{j}_i'' = -\Gamma \nabla y_i \tag{4}$$

where, $\Gamma = \rho D$. In the absence of Soret, pressure diffusion, and Knudsen effects, the governing equation can be written in the commonly-encountered form [15–19],

$$\frac{\partial}{\partial t}\left(\rho y_i\right) + \nabla \cdot \left(\rho \boldsymbol{U} y_i\right) - \nabla \cdot \left(\Gamma \nabla y_i\right) = 0 \text{ in } \Omega \tag{5}$$

Other quantities, such as concentration, may be entertained as dependent variables, as may alternative definitions of the mixture velocity in place of mass-averaged values, for computing relative flux. These will not be considered here. Also, from here on, the transient term in Eq. (5) will be dispensed with, in order to eliminate redundant terms unnecessary for the analysis. This may easily be recovered, if and when circumstances necessitate. Furthermore, for problems involving homogeneous chemical or nuclear reactions, the right-sides of Eqs. (1), (3), (5) are not zero, however that does not alter the following discussion.

2.2. Boundary conditions

The convention followed here is that the boundary fluxes are positive for injection and negative for suction, i.e., $\dot{m}_i'' = -\dot{\boldsymbol{m}}_i \cdot \hat{\boldsymbol{n}}$, $j_i'' = -\boldsymbol{j}_i \cdot \hat{\boldsymbol{n}}$ etc., where $\hat{\boldsymbol{n}}$ is the outward unit normal to $\partial\Omega$, see Fig. 1. There are at least three possible ways to prescribe BCs for Eq. (5), on the surface of the external boundary, $\partial\Omega$. These are given below in Eqs. (6)–(8).

$$j_i'' = \dot{m}_i''\left(1 - y_i\right) - \sum_{k \neq i} \dot{m}_k'' y_k \quad \text{on } \partial\Omega \tag{6}$$

$$j_i'' = \sum_{k \neq i} \left(\dot{m}_i'' y_k - \dot{m}_k'' y_k\right) \quad \text{on } \partial\Omega \tag{7}$$

$$j_i'' = \dot{m}''\left(y_{i,T} - y_i\right) \quad \text{on } \partial\Omega \tag{8}$$

$$y_{i,T} = \frac{\dot{m}_i''}{\dot{m}''} \tag{9}$$

Eq. (8) is the form of the CMTBC preferred in this paper: $y_{i,T}$ is the T-state value [2,16,19] for substance i. The name refers to the fact that one or more species is/are selectively transferred across the boundary $\partial\Omega$. The T-state is sometimes introduced in the context of filtration, as an external or far-field condition; where diffusion gradients are negligibly small, with $0 \leq y_T \leq 1$ for each species. Fig. 2(a) illustrates the problem schematically. A simple example would be the injection or extraction of pure water to/from a mixture of ethanol and water, or injection of pure hydrogen gas into, say, helium, Fig. 2(b). Transfer could be across a membrane located at the boundary, B, that is selectively permeable. Fig. 2(c) illustrates another example, namely a heterogeneous electrochemical reaction [6], namely the redox reaction in a solid oxide fuel cell, where hydrogen molecules, $2H_2$, combine with O^{2-} ions to produce water vapor, $2H_2O$, and electricity, $4e^-$. The overall mass flux of all species, $\dot{m}''$ (the sum of H_2 and H_2O), is into the region Ω (positive), whereas the flux of H_2, $\dot{m}_{H_2}''$ is out of Ω (negative). For problems involving heterogeneous chemical reactions, $-\infty \leq y_T \leq +\infty$, for the case shown Fig. 2(c); for H_2O, $y_T = +9/8$, and for H_2, $y_T = -1/8$, assuming the molecular weights to be (approximately) 18 and 2. Chemical catalysis, where $\dot{m}'' = 0$ but $\dot{m}_i'' \neq 0$ and therefore $y_T = \pm\infty$ (not shown) is an important special case. In the context of chemically reacting flows, the T-state is not an actual mass fraction, but rather a convenient device for problem formulation. The first term in Eq. (6) is the increase (or decrease) in y_i due to injection (or extraction) at rate $\dot{m}_i''$ of species i. The second term is the decrease (increase) in y_i due to injection (extraction) at rate $\dot{m}_k''$ of species k, $k \neq i$, balancing the associated change of y_k. Even though Eqs. (6)–(7) may be functionally equivalent to Eq. (8), they suffer from several practical disadvantages:

(i) y_k appears in the equation for y_i; unnecessary and potentially unstable.
(ii) For binary diffusion, there is one equation with two terms to be solved; for ternary diffusion, two equations with three terms each, etc.; whereas for Eq. (8) there is a single BC.

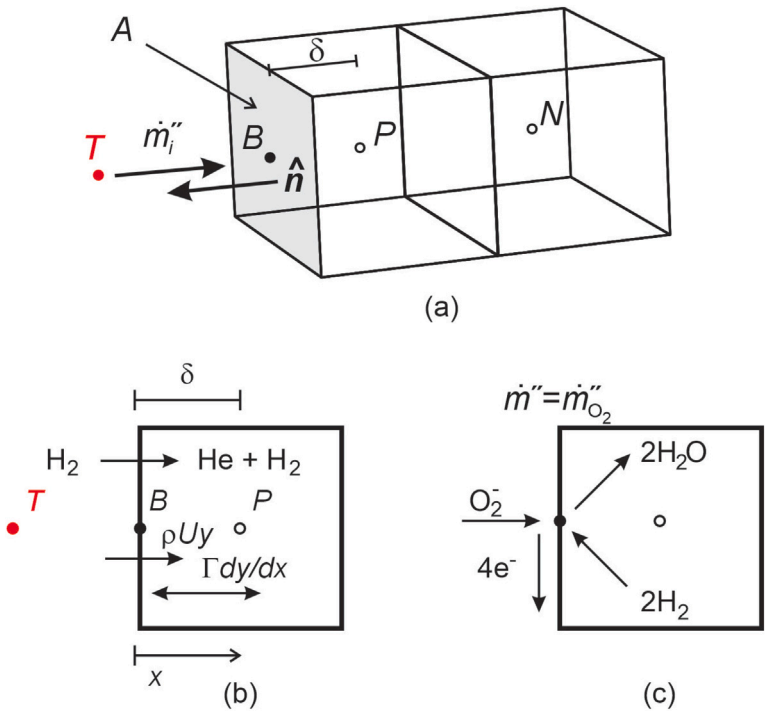

Fig. 2. Conceptualization of the mass transfer boundary value problem illustrating: (a) geometry and nomenclature; (b) simple membrane filtration convection–diffusion problem, where pure hydrogen is injected into a binary mixture of hydrogen and helium; (c) heterogeneous electrochemical reaction where oxygen ions react with hydrogen to produce water and electrons.

(iii) The latter terms in Eqs. (6) (7) must be coded as Neumann BCs, whereas Eq. (8) may be linearized, at least for inflow.
(iv) The $\dot{m}_i''$ appearing in Eqs. (6), (7) are the individual species fluxes, whereas, $\dot{m}'' = \rho U_B$ in Eq. (8) is the overall/mixture convective mass flux, consistent with the usual treatment at inlets/outlets in CFD, obtained from the Navier–Stokes equations.

The reader will note that y_B is the boundary value of y, i.e., on the surface $\partial\Omega$, not the value, y_P, in the nearest computational cell within the finite volume, Ω, see Fig. 2(a). Similarly U_B is the mixture velocity just inside Ω. Henceforth, in the interests of brevity, the subscript 'i', for example y_i is excluded, it being understood that a number of individual species are being solved-for, and therefore where there is no ambiguity, the mass fraction, y_i, is denoted simply by y.

2.3. Dimensional and non-dimensional parameters

In the following sections; both the conventional mass transfer notation [19] and popular CFD/FVM symbols [17] are employed simultaneously. This may lead to some unavoidable duplication, but has the advantage of being self-contained and comprehensive in scope.

2.3.1. Cell level

A cell Spalding number or mass transfer driving force, B, may be defined at boundary cells according to,

$$B = \frac{y_P - y_B}{y_B - y_T} \tag{10}$$

Although this concept enjoys widespread application in the mass transfer literature [16,18,19]; it has not been introduced in the correspodning CFD literature, for example, [17,20–23]. The wall mass fraction may be computed from;

$$y_B = \lambda y_P + (1-\lambda)\, y_T \tag{11}$$

where

$$\lambda = \frac{1}{B+1} \tag{12}$$

is a weighting function. The boundary value, y_B, is not constant, but a function of the local in-cell value, y_P. y_B is bounded by y_P and y_B provided $0 \le \lambda \le 1$, but not otherwise. The cell Spalding number, B, is considered a function of the cell Péclet number, P, or cell blowing parameter,

$$P = \frac{F}{D} = \frac{\rho U_B \delta}{\Gamma} = \frac{\dot{m}''}{g^*} \tag{13}$$

F and D are the convection and diffusion coefficients, Patankar [17].

$$F = A\rho U_B \tag{14}$$

$$D = A\frac{\Gamma}{\delta} \tag{15}$$

It is to be noted that D is based on the diffusion flux in the limit $\dot{m}'' \to 0$. For 1-D convection–diffusion, $g^* = \Gamma/\delta$, is the corresponding limiting or film conductance. The actual conductance, g, at finite $\dot{m}''$, may be greater or less than g^*, due to the effects of convection. $\delta = |\boldsymbol{d}_{BP}|$ is the node-to-boundary distance, and A is the area of the cell boundary, see Fig. 2(a). The reader will note that, in the interests of readability, a structured hexahedral geometry is illustrated in Fig. 2; however there is no problem in considering unstructured polyhedral meshes where $\boldsymbol{d}_{BP}$ is not parallel to the face normal, $\hat{\boldsymbol{n}}$ [24].

The total flux at the cell boundary, $\partial\Omega$, is the sum of the convective and diffusive contributions,

$$j''_{\mathrm{TOT}} = \dot{m}'' y_T = \dot{m}'' y_B + g(y_B - y_P) \tag{16}$$

N.B.: $j''_{\mathrm{TOT}} = j''_{\mathrm{TOT},i} = \dot{m}_i''$ is the individual species not the overall/mixture flux $j''_{\mathrm{TOT}} \neq \dot{m}''$. The fundamental relationship for mass transfer [2,16] may be written as follows,

$$\dot{m}'' = g\,B \tag{17}$$

or in non-dimensional form:

$$P = \frac{g}{g^*} B \tag{18}$$

Eq (18) relates three non-dimensional parameters, B (driving force or potential), g/g^* (non-dimensional conductance), and P (non-dimensional mass flux). The cell conductance, $g = j''/(y_B - y_P)$, is the ratio of the diffusion flux at the cell interface to the difference in wall and interior mass fractions: which may written, $j'' = \lambda \dot{m}'' \left(y_T - y_P\right)$. The weighting factor, $\lambda = 1/(B+1)$, is the ratio of the rate of mass transfer by diffusion alone to mass transfer by both convection and diffusion. It remains to eliminate the unknown driving force, B, by means of some suitable closure.

2.3.2. Non-dimensional numbers on the macroscopic scale

Péclet and Spalding numbers are defined in standard mass transfer texts. Macroscopic values are denoted here with a tilde, $\tilde{P}$, $\tilde{B}$, rather than the cell-level definitions which have no tilde. Typically $\tilde{P} = Re \cdot Sc$ for mass transfer or $\tilde{P} = Re \cdot Pr$ for heat transfer. This does not directly correspond to the cell-scale definition above, as the reference velocity is a free stream value rather than value normal to the boundary surface. However Patankar [17] and numerous subsequent authors, make reference to the cell Péclet number in the present form. A better correspondence is to be had with the macroscopic blowing parameter, $\tilde{b} = \dot{m}''/\tilde{g}^*$. The macroscopic Spalding number, $\tilde{B}$, is associated with the fundamental mass balance, $\dot{m}'' = \tilde{g}\tilde{B}$, where $\tilde{g}$ is a local or overall mass transfer coefficient.

2.4. Steady one-dimensional laminar convection–diffusion

Returning to the cell-level problem: Starting from a 1-D constant property convection–diffusion equation,

$$\rho U y - \Gamma \frac{dy}{dx} = \rho U y_T \tag{19}$$

with $y = y_B$ at $x = 0$ and $y = y_P$ at $x = \delta$, Fig. 2(a). y_P is the interior nodal value of y within Ω, adjacent to $\partial\Omega$. The solution to Eq. (19) may accordingly be written;

$$B = \exp P - 1 \tag{20}$$

$$\frac{g}{g^*} = \frac{\ln(1+B)}{B} = \frac{P}{\exp P - 1} \tag{21}$$

2.5. Linear algebraic equations

The finite volume equations are obtained from a flux balance and may be written in the following zero-residual form,

$$\left(\sum_N F_n\right) y_P + \sum_N a_N \left(y_N - y_P\right) + S = 0 \tag{22}$$

where N is the number of cell faces. Overall continuity dictates that the first term of Eq. (22) is zero, and it is normally excluded from texts, but it is retained in Eq. (22) in parenthesis, as a reminder that the boundary flux balance must implicitly include a convective term, F_W, as well as a diffusive term, for the fluxes to sum to zero.

The system may be expressed in vector-matrix form:

$$\mathbf{a} \cdot \mathbf{y} = \mathbf{b} \tag{23}$$

2.6. Classification of codes

Fig. 3 illustrates some of the CFD rationales employed. Many codes employ a cell-centered rationale, Fig. 3(a)–(c). In codes, such as `OpenFOAM` [25], an additional boundary mesh is constructed around the periphery, Fig. 3(a). Other finite-volume codes, for example `PHOENICS` [26], do not employ boundary meshes, see Fig. 3(b). This is the approach suggested by Patankar [17] and employed in numerous user-written codes. In some cases, additional 'halo' or 'ghost' cells may be introduced as shown in Fig. 3(c). In codes such as `StarCCM+` and `ANSYS CFX` a vertex-centered rather than a cell-centered scheme, Fig. 3(d), is used.

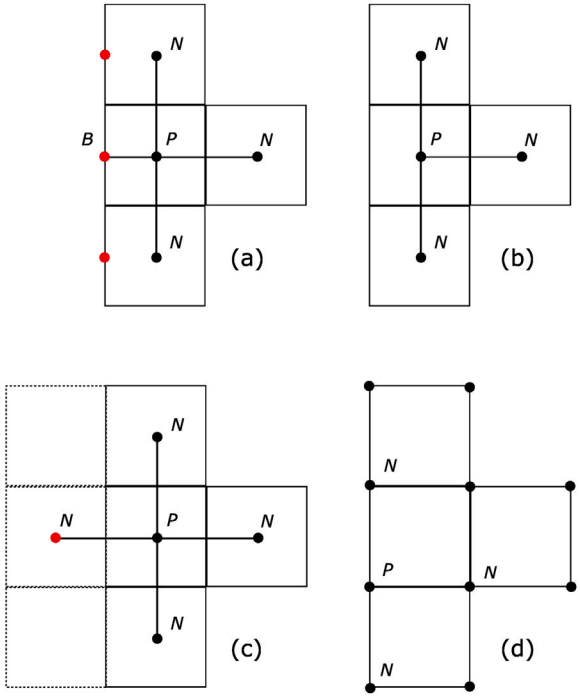

Fig. 3. Computational cell geometry: Cell-centered scheme with: (a) Stored boundary nodes. (b) No boundary nodes. (c) 'Halo' or 'ghost' cells. (d) Vertex-centered scheme.

2.7. Wall boundary conditions

For codes where the boundaries are included in the mesh, Fig. 3(a), the user provides the boundary values, y_B, (or flux/gradient); the wall coefficient, a_B, is computed using the same scheme as employed for interior neighbor coefficients, a_N, and the wall coefficients, a_B, are calculated internally. Eq. (24) differentiates internal N-terms and boundary B-terms as follows:

$$\sum_N a_N \left(y_N - y_P\right) = \sum_{N-N_B} a_N \left(y_N - y_P\right) + \sum_{N_B} a_B \left(y_B - y_P\right) \tag{24}$$

Multiple conditions $N_B > 1$, are applied at sub-regions or 'patches' of the boundary mesh, e.g., at edges/corners etc. In the interests of readability, however, let it be assumed henceforth a given cell is associated with just a single wall value, $N_W = 1$. If B follows Eq. (20), then the boundary values and fluxes at point W are computed according to Eqs. (11) with $\lambda = \exp(-P)$. Eq. (16) may be written

$$j''_{\mathrm{TOT}} = \left(\dot{m}'' y_P\right) + (\dot{m}'' + g)(y_B - y_P) \tag{25}$$

Thus, the wall coefficient is of the form,

$$a_B = A(g + \dot{m}'') \tag{26}$$

For an exponential difference scheme (EDS) [17],

$$\frac{a_B}{D} = \frac{g}{g^*} + P = P\frac{\exp(P)}{\exp(P) - 1} \tag{27}$$

and not $a_B = Ag$ because of the presence/requirement of the convective term (in parenthesis; the first term in the flux balance, Eq. (22)).

Should a different scheme from the EDS be chosen, the wall value prescription, Eq. (11), can be modified based on the new B (or g/g^*) distribution. Expressions for B, g/g^*, and λ for some popular numerical schemes, such as the central (CDS), upwind (UDS) [27], and hybrid (HDS) schemes [28] are presented in Table 1. Other schemes can be considered; for instance Perić [29] proposed a blended differencing scheme, $y = (1-\gamma)y_{\mathrm{UDS}} + \gamma y_{\mathrm{CDS}}$. Numerous higher-order schemes [30] have been devised which trade-off between accuracy and stability, in particular when the flow is not oriented with the mesh.

2.8. Source term formulation

Many finite-volume codes [17], for example PHOENICS [26], do not employ boundary meshes, but rather add a source-term, corresponding loosely to a Robin (linear) condition, see Fig. 3(b). In Spalding's notation [11], the source term is composed of a source term coefficient, C, and a value, V.[1]

$$S = C\left(V - y_P\right) \tag{28}$$

which mimics the missing a_B and y_B terms, Eq. (22), above. Patankar [17] employed a similar approach, with slightly different notation,

$$S = S_C + S_P y_P \tag{29}$$

which has been widely adopted. Under the circumstances:

$$y_P = \frac{\sum_N a_N y_N + CV}{a_P} = \frac{\sum_N a_N y_N + S_C}{a_P} \tag{30}$$

$$a_P = \left(\sum_N F_n\right) + \sum_N a_N + C = \left(\sum_N F_n\right) + \sum_N a_N - \frac{S_C}{S_P} \tag{31}$$

The user must provide both the coefficient and the value, rather than just the boundary value.

2.8.1. Convective mass transfer boundary condition

From Fig. 2(a) it is seen that the total rate of mass transfer of the transferred substance at the boundary is,

$$j_{\mathrm{TOT}} = F y_T = F y_P + F\left(y_T - y_P\right) \tag{32}$$

Thus, the CMTBC boundary condition is,

$$\begin{aligned} C &= F \\ V &= y_T \end{aligned} \tag{33}$$

whereas in Patankar's notation, Eq. (29),

$$\begin{aligned} S_P &= -F \\ S_C &= F y_T \end{aligned} \tag{34}$$

Eqs. (33) and (34) are linear forms suitable for inflow, with $F > 0$, the C-term (S_P term) appears in the diagonal of the **a** matrix and the CV-term (S_C term) in the **b** vector, Eq. (23). For net outflow, $F < 0$, a fixed source $S = C(V - y_P)$ or $S = S_C + S_P y_P$ is placed on the right-side in the **b** vector, Eq. (23), to conform to the rule of positive source term coefficients [17]. One approach to achieve this is to set $C = 10^{-10}F$, and $V = 10^{10}F(y_B - y_P)$. (There is nothing special about $10^{\pm 10}$. Any suitably small/large number combination may be employed.)

2.8.2. Wall boundary condition

If, instead, a wall boundary mesh is employed, Fig. 3(a),

$$j_{\mathrm{TOT}} = F y_P + D\left(P + \frac{g}{g^*}\right)\left(y_B - y_P\right) \tag{35}$$

For an EDS

$$\begin{aligned} C &= F\frac{\exp P}{\exp P - 1} \\ V &= y_B \end{aligned} \tag{36}$$

$$\begin{aligned} S_P &= -F\frac{\exp P}{\exp P - 1} \\ S_C &= F\frac{\exp P}{\exp P - 1} y_B \end{aligned} \tag{37}$$

where from Eq. (11)

$$y_B = \exp(-P)\, y_P + \left[1 - \exp(-P)\right] y_T \tag{38}$$

[1] In some works a geometric factor, G, is included, i.e., $S = GC\left(V - y_P\right)$.

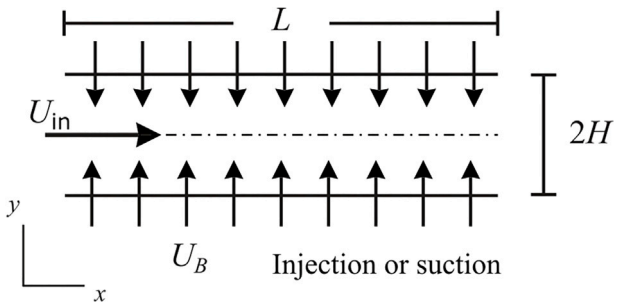

Fig. 4. Idealized schematic of 2-D plane duct problem (not to scale).

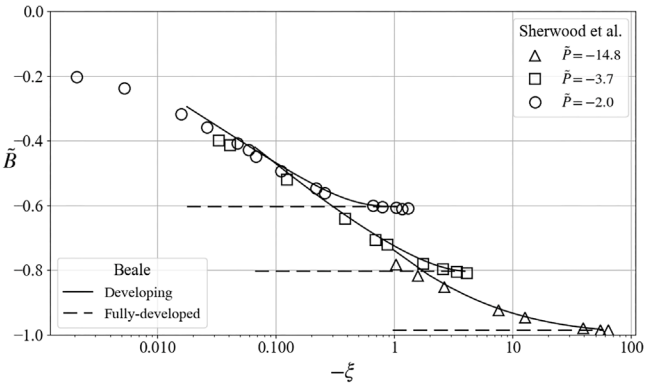

Fig. 5. Comparison of the results CFD calculations [3] based on the CMTBC, with those of Sherwood et al. [34] for developing and fully-developed mass transfer in a planar geometry. Macroscopic driving force/Spalding number, $\tilde{B}$, is shown as a function of non-dimensional displacement, ξ.

The source term calculated according to Eq. (28) based on the coefficients and values in Eq. (36) is identical to that based on Eq. (33), namely, $S = F(y_T - y_P)$, which is true for all consistent formulations with non-zero coefficients, not just the exponential scheme, Eq. (20), above. The key difference is that both the wall coefficient and value are prescribed, rather than only the value. It is worth noting that one can always convert a code where the BCs are prescribed as source terms, Fig. 3(b), into the same form as Fig. 3(a), simply by adding a set of additional set of boundary or 'halo' cells, Fig. 3(c), and subsequently applying a Dirichlet condition at the nodes of the boundary cells. Conversely, for codes like OpenFOAM where wall BCs must be prescribed, a zero flux/gradient Neumann condition may be prescribed at the relevant boundary patch(es), and an additional source term added.

2.9. Validation and verification

The CMTBC has been implemented by the present author and others in several mass transfer applications, including membrane passages [3, 4], and electrocatalysis problems [31–33]. Fig. 4 is a schematic of a simple plane duct. Fig. 5 shows a comparison of CFD calculations based on the CMTBC [3], with those of Sherwood et al. [34]. Results are presented in terms of a macroscopic Spalding number, $\tilde{B}$, versus non-dimensional distance, $\xi = 4U_B\tilde{P}^2/3U_0D_h$, for developing and fully-developed regimes. It can be seen that for developing mass transfer, agreement between the CMTBC results and the calculations of Sherwood et al. [34] is good. For strong suction, $\tilde{P} = -14.8$ and $\tilde{B} \to -1$, fully-developed conditions may not be reached before all the permeate is extracted and $y_B \to 0$. These results show that the CMTBC, Eq. (8), coded via Eqs. (33)/(34), generates reliable data when compared to independently obtained results.

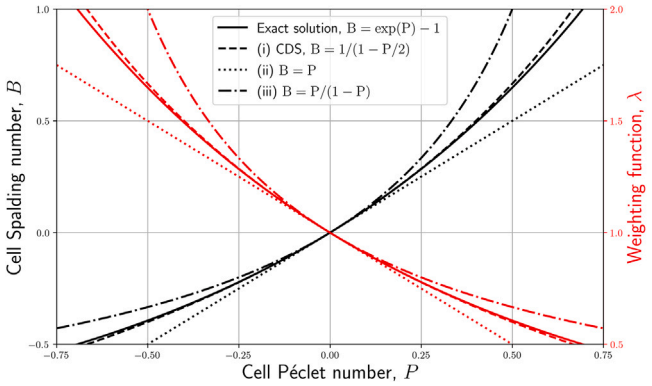

Fig. 6. Low mass transfer. Left ordinate (black lines): Cell Spalding number, B, for various approximations. Right ordinate (red lines): cell weighting factor, λ. (For interpretation of the references to color in this figure legend, the reader is referred to the web version of this article.)

3. Popular cell level schemes

3.1. Low mass transfer rates: $|P| \ll 1$

Numerical integration schemes generally do not employ exponential terms, because of computational expense, and moreover the EDS is only exact for a 1-D constant property solution. Mass transfer problems often involve injection/suction to flowing fluids at very low transfer rates, corresponding to $|P| \ll 1$. The exact/exponential difference scheme (EDS) Eq. (20), may be replaced by a simple linear expression, for example:

(i) The function g/g^*, Eq. (21), may be expanded in a Taylor series, $g/g^* = 1 - P/2\,(+P^2/12 + \cdots)$ and truncated at $O(P^2)$, consistent with a central difference scheme (CDS). The Spalding number is given in Table 1 as $B = P/(1 - P/2)$, and y_B calculated from Eq. (11) with $\lambda = (1 - P/2)/(1 + P/2)$ in place of $\lambda = \exp(-P)$.

(ii) Another approximation is to expand $B = P\,(+P^2/2 + \cdots)$, so that $\lambda = 1/(1 + P)$ in Eq. (11). This approximation is commonly-made for low rate problems [18]. The physical interpretation is of convection and diffusion 'resistances in series'. Note that while D is always positive F is not. For the case, $y_P \approx 0$, $y_T \approx 1$, $\dot{m}'' = g(y_B - y_P)$.

(iii) Alternatively expand λ with $\exp(-P)$ as $1 - P$, so that $B = P/(1 - P)$.

Cases (i)–(iii) are compared graphically with the EDS in Fig. 6. Case (i), CDS, agrees well with the exponential solution with B values slightly lower for $P < 0$ and higher for $P > 0$. For case (ii) values are lower for all P whereas for (iii) they are significant higher than the exponential solution. All cases are identical in the limit $P \to 0$, $B \to P$. The reader will note that for $P \neq 0$ the deviations between the exact 1-D EDS solution and case (ii), the linearized formula $B = P$, which enjoys widespread use in low-rate mass transfer theory [18], are greater than for the CDS. Case (iii) is not generally employed.

For the filtration example, Fig. 4, the maximum macroscopic Péclet number based on channel width H is $\tilde{P} = -14.8$, the minus sign indicating suction. The cell Péclet number is just $P = (H/\delta)\tilde{P}$. For the mesh employed in ref [3], δ/H is less than 0.001, i.e., B is very small. In general when fine meshes are concentrated near walls, a low mass transfer rate can be safely assumed. However, at the inlet to a turbulent flow problem, one can anticipate Reynolds number to be $O(10^6)$ and $|P| \gg 1$ may be encountered.

3.2. High rate mass transfer

Fig. 7 (left side, black), is a plot of cell Spalding number, B, as a function of cell Péclet number, P, for various schemes. Values of the weighting function, λ, are displayed on the right side, in red. Fig. 8 shows the normalized diffusion coefficient, g/g^*, (similar to that shown in Fig. 5.4 and 5.6 in [17]). Also shown is the wall coefficient, $a_B/D = g/g^* + P$. Algebraic expressions are given in Table 1. It is seen from Fig. 7 that the exact EDS ranges from $B = -1$ as $P \to -\infty$, to $B = +\infty$, as $P \to +\infty$. None of the other schemes displayed, namely upwind/central/hybrid difference schemes (henceforth referred to as UDS, CDS, HDS) agree particularly well with the EDS. This has nothing to do with the mesh orientation being at an angle to the flow, as is typically considered with investigations on so-called 'higher-order schemes', [30,35,36] but rather the UDS, CDS, HDS etc. are simply poor approximations.

The UDS overpredicts B for $P \leq 0$ and underpredicts for $P \geq 0$, in comparison to the EDS. Comparison of the UDS values in Table 1 and the results of Fig. 6 (low mass flow) reveals the B-profile based on the UDS scheme is the same as case (ii) $B = P$ for $P \geq 0$ and case (iii) $B = P/(1 - P)$ for $P < 0$. The HDS and CDS are identical for $-2 \leq P \leq 2$. The HDS/CDS underpredict B for $P \leq 0$ and overpredict for $P \geq 0$, but display somewhat better agreement with the EDS than the UDS, at least in the range $-2 \leq P \leq 1$, with errors in B accumulating as $P \to 2$, $B \to \infty$ according to the HDS/CDS, whereas for the EDS $B = \exp(2) - 1 = 6.39$, is always finite, and continues to increase for $P > 2$. The corresponding value of $g/g^* = 2/(\exp(2) - 1) = 0.31$, is shown in Fig. 8, whereas $g/g^* = 0$ according to the HDS/CDS at $P = 2$. This means the linear coefficient, a_B, has no component due to diffusion with $a_B = F$. Values of B for the CDS with $P > 2$ are actually negative, implying counter-gradient diffusion, i.e., not physically realistic. Also for the CDS, values of $P < 2$ generate $B < -1$, which is also not realistic.

Values of the weighting function, λ, mirror the B-distribution, but with λ ranging from 0 to 1 for positive values of P, and from 1 to ∞ for negative P-values. It can be seen that as $P \to 0$, $\lambda \to 1$, so that from Eq. (11) $y_B \to y_P$ i.e., is independent of y_T. For the HDS; computed values of y_B based on λ, Eq. (11), will exhibit large deviations from the EDS around $P = 2$, see Fig. 7. With $P \leq -2$, $\lambda = \infty$ and with $P \geq +2$, $\lambda = 0$.

For negative P; $g/g^* > 1$ indicates that the mass transfer conductance increases for suction (outflow) and conversely for $P > 0$; decreases for injection (inflow). Normalized values of the wall coefficient, $a_B/D = g/g^* + P$, indicate the influence of the upstream wall value to be large for blowing ($P > 0$) and negligibly small for strong suction ($P \ll 0$).

The HDS fixes $B = -1$ for $P \leq -2$, which completely cuts out all diffusion for suction (outflow) with $a_B = 0$. This means that mass transfer at the boundary will be completely cut-off, if a wall value prescription rather than the CMTBC is employed. No matter what boundary value, y_B, is prescribed, it will have no influence on the interior value, y_P. For high-mass transfer suction, the wall approach will fail to capture boundary mass transport. The CMTBC prescription does not suffer from this defect. The HDS has been the subject of criticism [35,36] for reasons aside from mass transfer limits. Diffusion at the boundary is also cut-off for injection/blowing at the boundary with $a_B = A\dot{m}''$, i.e., transport by convection, alone; the coefficient is the same as the CMTBC but the value is the wall value, which is clearly incorrect, since $y_B \neq y_T$ as implied by the incorrect identity $B = \infty$ for $P = +2$.

3.3. Other schemes

It is seen that the basic schemes (CDS, UDS, HDS etc.) differ substantially from the exact EDS for steady 1-D mass transfer. Higher-order convection schemes, such as the Quadratic-Upwind Interpolation

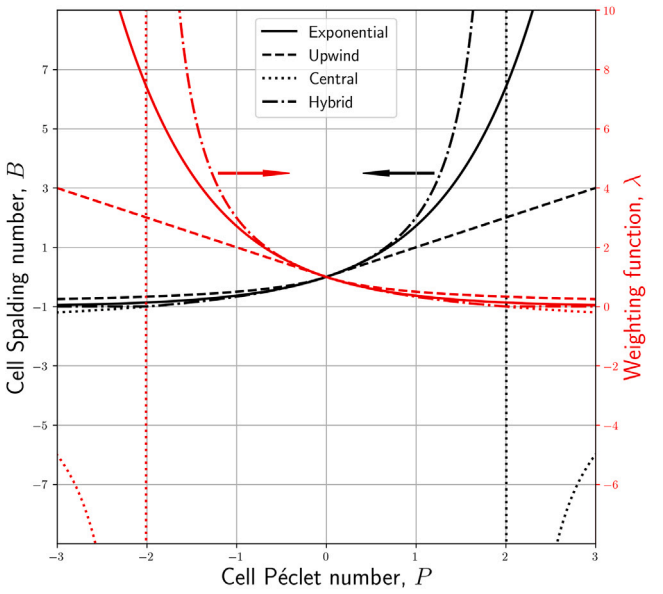

Fig. 7. High mass transfer. Left ordinate (black curves): Cell Spalding number, B. Right ordinate (red curves): cell weighting factor, λ. In the range $-2 \le P \le 2$ the central-difference and the hybrid schemes are identical. (For interpretation of the references to color in this figure legend, the reader is referred to the web version of this article.)

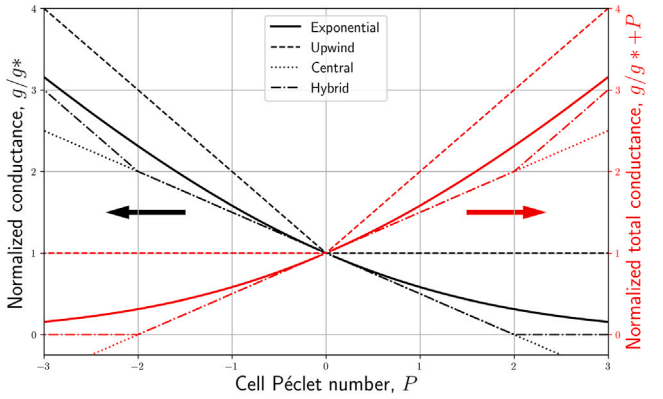

Fig. 8. Left ordinate (black curves): Normalized cell diffusion conductance, g/g^*. Right ordinate (red curves): Normalized total coefficient, $a_B/D = g/g^* + P$. (For interpretation of the references to color in this figure legend, the reader is referred to the web version of this article.)

scheme for Convective Kinematics (QUICK) [37], Total-Variation Diminishing (TVD) schemes [38], Monotonic UpStream-Centered Schemes for Conservation Laws (MUSCL) [39], and blended schemes [29] all enjoy widespread application as alternatives to the basic schemes presented here. These are generally concerned with minimizing numerical diffusion, e.g., when the flow and the mesh are misaligned. The general trade-off is between stability/boundedness and resolution. Waterson and Deconinck [30] discuss the relative merits of many such schemes.

Higher order convection schemes are not generally devised with actual/true diffusion, in particular at boundaries, in mind. Accuracy of the Spalding number, B, vs. Péclet number, P, profile is not generally considered. A complete set of cases corresponding to Figs. 7–8 for higher-order schemes would prove meritorious, as would efforts to devise further 2-D and 3-D convection–diffusion benchmarks compared to the idealized 1-D formulation given here. Table 1 is thus to be considered a first step in that direction, based on the most basic

Table 1
Spalding number, B, normalized conductance, g/g^*, and weighting function, λ.

	Exponential (EDS)	Upwind (UDS)		Central (CDS)	Hybrid (HDS)	
B	$\exp P - 1$	P $P/(1-P)$	if $P \ge 0$ if $P < 0$	$\frac{P}{1-P/2}$	∞ $\frac{P}{1-P/2}$ -1	if $P > 2$ if $-2 \le P \le 2$ if $P < -2$
g/g^*	$P/(\exp P - 1)$	1 $1-P$	if $P \ge 0$ if $P < 0$	$1-P/2$	0 $1-P/2$ $-P$	if $P > 2$ if $-2 \le P \le 2$ if $P < -2$
λ	$\exp(-P)$	$1/(P+1)$ $1-P$	if $P \ge 0$ if $P < 0$	$\frac{1-P/2}{1+P/2}$	0 $\frac{1-P/2}{1+P/2}$ $-\infty$	if $P > 2$ if $-2 \le P \le 2$ if $P < -2$

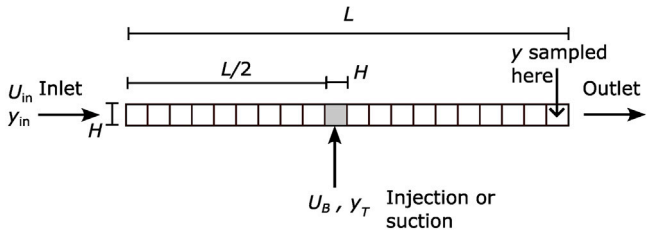

Fig. 9. Schematic of 1+1D T-branch problem.

schemes. Nevertheless, if the CMTBC rather than a wall value prescription is selected; regardless of the chosen numerical scheme, the correct source at the boundary will be applied. Conversely; when a wall value is calculated or prescribed during the computational procedure, it is important that the extrapolation method be consistent with the scheme employed. The matter is discussed further below.

4. Error analysis

4.1. Illustrative 1+1D problem

The importance of suitable implementation of mass transfer BCs is further illustrated with a simple 1+1D numerical benchmark. Consider the geometry shown in Fig. 9 where the main flow in the streamwise direction is augmented by mass transfer (injection/extraction) in a lateral branch across a small fraction of the boundary, thereby facilitating large P values to be attained, while ensuring that $0 \le y_P \le 1$ for all values of U_B. A mesh of $20 \times 1 \times 1$ cells is selected with an inlet mass fraction of $y_{in} = 0.5$. The procedure is as follows:

(i) The CMTBC, Eq. (8), was implemented with $S = F\left(y_T - y_P\right)$ with the coefficient based on the convection flux, $C = A\rho U_B$, Eq. (33), or $S_P = -A\rho U_B, S_C = A\rho U_B y_T$, Eq. (34).
(ii) A wall value for y_B was computed according to Eq. (11), with $\lambda = \exp(-P)$. The coefficient was then computed from $g/g^* + P$ according to the EDS, UDS, CDS, HDS, but the same exponential y_B.
(iii) Both the wall values of y_B as well as the coefficients, were varied in pairs, according to the EDS, UDS, CDS, HDS, see Table 1.

The finite-volume computer code PHOENICS [26] was employed. Similar results were obtained in comparisons of PHOENICS with the open source code OpenFOAM. A hybrid-scheme was employed for interior values. The error between the cases is tabulated as;

$$\epsilon = \frac{y_{\text{scheme}} - y_{\text{in}}}{y_{\text{CMTBC}} - y_{\text{in}}} \tag{39}$$

where y_{CMTBC} is the downstream value of y for case (i) above, and y_{scheme} is the downstream value for the cases (ii) and (iii), i.e., y_{EDS}, y_{UDS}, y_{CDS}, y_{HDS}.

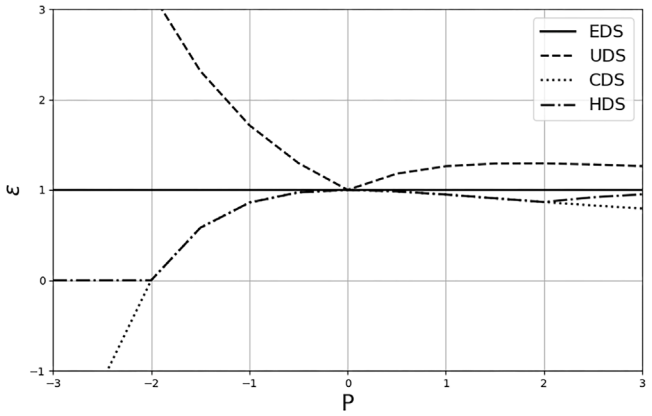

Fig. 10. Error, ϵ, in downstream mass fraction, for wall formulations compared to the CMTBC approach. The coefficient is varied, but the wall value is fixed.

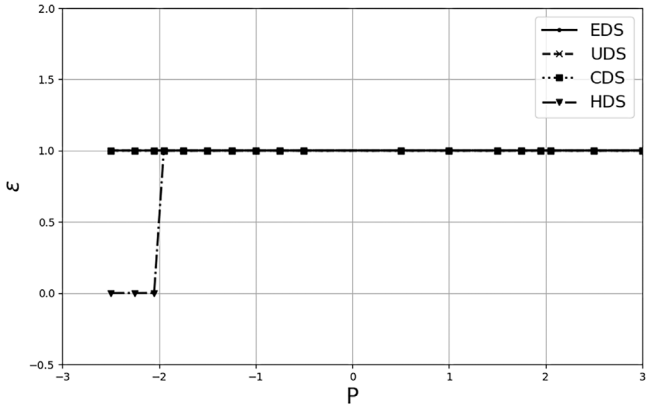

Fig. 11. Error, ϵ, in downstream mass fraction, for wall formulations compared to the CMTBC approach. The source term coefficient and value are both computed according to the same scheme.

Fig. 10 shows the normalized deviation from the CMTBC solution, Eq. (39), for each of the schemes given in Table 1, for case (ii). It can be seen that agreement between the exponential wall and the CMTBC formulation is exact, with $\epsilon = 1$, for all values of the Péclet number, P. The same cannot, however, be said for the other schemes. This is because the wall coefficient and value are not computed in a mutually consistent manner. The boundary coefficients are computed as $C = A(g + \dot{m}'')$, see Fig. 8. The larger coefficients noted for the UDS ensure that the in-cell mass fraction is closer to the boundary/wall value, thereby resulting in $\epsilon \geq 1$, i.e., an overprediction of diffusion effects. Conversely for the CDS and HDS, the boundary coefficients are less than for the EDS, resulting in values of $\epsilon \leq 1$. For $P \leq -2$ the HDS cuts out diffusion entirely. For $P \leq -2$ the CDS generates negative coefficients (Fig. 8) with meaningless results. This demonstrates the errors that can arise when the user specifies a wall value but the boundary coefficient is computed internally.

These errors do not arise if the boundary value is also computed using the same scheme, as the source term coefficient. This is true even if the boundary formulation differs from the scheme used for interior cells. Fig. 11 shows the errors, for this set of cases. With few exceptions, $\epsilon = 1$. Exceptions are seen to be the HDS for $P \leq -2$ and CDS for $P = -2$, depending on how floating point errors are error trapped. The source term coefficients are $C = 0$ for $P = -2$ (CDS), and for $P < -2$ (HDS). Otherwise, for all other cases, the wall formulation generates the same boundary source term as the CMTBC formulation in the converged state.

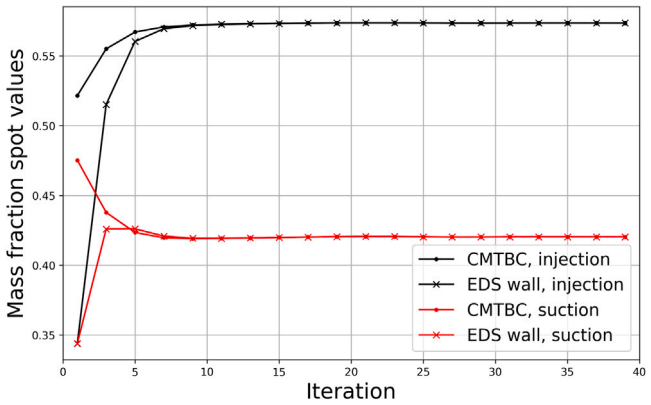

Fig. 12. Spot values for mass fraction, y, for values obtained using the CMTBC and a wall formulation. $\tilde{P} = \pm 0.65$.

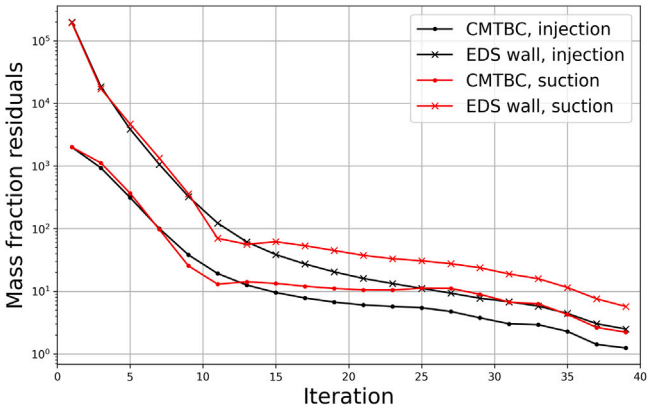

Fig. 13. Residuals for mass fraction, normalized with respect to a reference of 10^{-10} for values obtained using the CMTBC and a wall formulation.

In conclusion, the user needs to be aware that if they change the numerical scheme employed internally in commercial or open source CFD codes where a wall value must be prescribed, case Fig. 3(a) at run-time, then they must also change the boundary value computation, in a consistent manner. In particular, if a linear relationship, $B = P$, is used to compute y_B, errors will arise for all but the smallest of P-values. It is always safer to employ the CMTBC in the form of Eq. (8).

One minor advantage of the wall prescription is the fact that most schemes, other than the CDS/UDS, ensure positive source term coefficients (negative in Patankar's notation), and may therefore be used to linearize the source term for suction, $P < 0$, with potential speed-up of convergence. However, this apparent advantage is offset by the need to repeatedly iterate on the wall value, thereby slowing convergence, as shown below. When employing the T-state boundary value; linearization is possible for inflow, $P > 0$, however for outflow, $P < 0$, convergence is assured if a fixed rather than a linearized source term is employed, obviating negative terms in the matrix equation, Eq. (23).

4.2. Spot values and convergence history for plane duct problem

Figs. 12 and 13 show spot values and residuals for a case similar to the problem shown in Fig. 5. A constant mass transfer BC is coded as:

(a) The CMTBC, Eq. (8), and
(b) A wall boundary approach with an exponential formulation.

A mesh size of 40 × 40 × 1 was employed. The initial field, and upstream BC mass fraction values were presumed to be $y = 0.5$. Inlet

velocities were prescribed according to the Berman profiles [3,40]. Identical results are obtained in terms of converged spot values for both injection and suction. If a wall value is coded a_B (or C) is always positive, however it is very small for negative P (suction/outflow), so that the wall term is small compared to neighbor terms. Spot value convergence is more rapid for the CMTBC than for the wall BC. The improvement is less significant for suction, though it can be seen that the residuals are substantially lower for the CMTBC than the wall approach. The wall values and coefficients change and require iteration, whereas for the CMTBC these are fixed. Conventional wisdom is that C should be positive in Eq. (28), i.e., S_p negative in Eq. (29) [17]. For $P < 0$, the source term should be coded as fixed flux (Neumann), i.e., in the **b** vector in Eq. (23) to satisfy Scarborough's criterion [41], $|a_P| \geq \sum_N |a_N|$, which is generally regarded as a rule-of-thumb; sufficient but not necessary. For values of $|P| \ll 1$, the linear form of Eqs. (28) (29) still results in convergence even if S_P is positive, when $P < 0$ (outflow). It is to be noted that for negative P, large negative values of C or large positive values of a_P do not in general arise, i.e., the boundary term is always smaller in magnitude than at least one other term in the finite-volume equation. Regardless, the CMTBC formulation exhibits a performance improvement in terms of convergence, as compared with the wall value formulation.

Of course cases will arise, e.g., in membrane technology and/or where chemical reactions are involved, where the mass flux is a function of the local concentrations, and iteration will then be required with the CMTBC formulation. The precise convergence history will depend on the details of how the **a**-matrix, Eq. (23), is assembled and exactly when the BCs are updated, which will vary from code-to-code. Nevertheless, the above calculations indicate the efficacy of the CMTBC approach, when compared to a wall-based approach.

5. General nature of the convective mass transfer boundary condition

5.1. Inlets, outlets and walls

Inlets, outlets and solid walls may all be considered to be particular instances of the CMTBC; not only for mass fraction, y, but for any generic scalar, ϕ, as variable; for example temperature, T, and even velocity.

5.1.1. Inlets

As $P \gg 1$, $B \to \infty$, $y_B \to y_T$, (upwind dominance) i.e., an inlet condition. Under the circumstances y_T is just the upstream value of y. The inlet condition encountered in CFD is just the same as the CMTBC.

5.1.2. Outlets

For $P \ll -1$, $B \to -1$ so that $y_B \to y_P$, $S \to 0$, for an outlet. The latter is often referred to, in a somewhat cavalier manner, as a 'zero gradient condition'. For the wall formulation, there are two distinct reasons why $S = 0$; (i) when the values are equal, $y_B = y_P$, and (ii) the source term coefficient, C or S_P, is very small for large negative values of P, see Eqs. (36)–(37). For both cases the CMTBC downstream value is just $y_T = y_P$. While the coefficient in a wall formulation can be very small, if it is zero, as previously discussed, relative mass fluxes cannot be captured at outlets. A mass-transfer outflow BC differs from the common fluid flow outlet, if the boundary is selective to the efflux of different species: The gradients and relative fluxes, are non-zero. A 'filtering' or 'sifting' of species occurs with holdback of the retained species.

5.1.3. Walls

A wall is the limiting condition as $\dot{m}'' \to 0$ for injection or suction. To prescribe a constant wall flux boundary (Neumann) condition, j'', simply fix $S = Aj''$. To prescribe this as the limit of a linear (Robin) condition, set $C = 10^{-10}A$ and $V = 10^{10}j''$ in Eq. (28), or $S_C = j''$, $S_P = -10^{-10}$ in Eq. (29). (N.B.: Any suitable pair of small/large numbers may be selected). A wall gradient, $\partial\phi/\partial n = -j''/\Gamma$, rather than a flux, may be similarly prescribed.

For constant wall value (Dirichlet condition); with $|P| \ll 1$, going to the limit $|P| \to 0$, $B \approx P$ and,

$$y_T = y_B + \frac{y_B - y_P}{P} \approx \frac{y_B - y_P}{P} \quad \lim\ P \to 0 \tag{40}$$

assuming some suitably small value for $\dot{m}''$. It immediately follows from Eq. (8) that $j_B'' \to (\Gamma/\delta)\left(y_B - y_P\right)$ which is the usual laminar-type BC, in the absence of injection/suction at the wall. Assuming $F = 10^{-10}$ and $C = 10^{-10}$, $V = 10^{+10}D\left(y_B - y_P\right)$. In Patankar's notation this corresponds to $S_C = D\left(y_B - y_P\right)$ and $S_P = -10^{10}$.

For a heterogeneous chemical reaction, such as catalysis where $y_T \to \pm\infty$ as $\dot{m}'' \to 0$, but the individual $\dot{m}_i'' \neq 0$.

$$\sum_i^{\text{Reactants}} a_i R_i \to \sum_j^{\text{Products}} b_j P_j \tag{41}$$

where a_i, b_i are the stoichiometric coefficients for reactants R_i and products P_j. The T-state values for individual reactants/products are easily computed from the products of the stoichiometric coefficients and molar masses of the components. If the mass flux of reactant i may be written,

$$\dot{m}_i'' = -k_i \prod_j^{\text{Reactants}} y_j^{\gamma_j} \tag{42}$$

where k_i is the reaction rate for species i, and γ_j are the reactant orders. Then the boundary value would be prescribed, as above, by setting $j_i'' = g^*(y_B - y_P)$. This again may be achieved by setting $C = 10^{-10}A$ and $V = 10^{+10}\dot{m}_i''$. Similar treatment may be accorded to products. Of course any suitable kinetic expression may be substituted for Eq. (42). If, however $\dot{m}'' \neq 0$, see Fig. 2(c), then the CMTBC may be applied directly.

5.2. Boundedness and limiting flux

It is important to appreciate that y_B is not necessarily bounded by y_P and y_T, depending on the value of y_T, U, and y_P. For injection of a single pure substance $U > 0$, $y_T = 1$ and $y_P < y_B < y_T$ (bounded), however for suction $U < 0$, $y_T = 1$, but $y_B < y_P < y_T$ (not bounded). This is indicated by values of the weighting factor, λ; For $P \geq 0$, $0 < \lambda \leq 1$ whereas for $P < 0$, $\lambda > 1$.

The situation is further complicated by the fact that y_T is not confined to the range $(0, 1)$. However, in general, if $P > 0$, then $B > 0$ and y_B is bounded by y_T and y_P, however if $P < 1$, it no longer is. y_B must, of course, always lie in the range $(0, 1)$. Conversely y_T frequently does not represent an actual mass fraction value; rather if $\dot{m}''$ [kg/m^2] total mass is added or removed then $\dot{m}''y_T$ [kg/m^2] of the transferred species is added or removed, i.e., the individual fluxes are correct.

For suction, $P < 0$, a limiting mass flux, or velocity, U_{lim}, is obtained when $y_B = 0$ and $B_{\text{lim}} = -y_P/y_T$ and hence from Eq. (20) $P_{\text{lim}} = \ln\left(1 - y_P/y_T\right)$. If $|y_p/y_T| \ll 1$ then the further simplification $P_{\text{lim}} = -y_P/y_T$ can be made. This provides a limit on the boundary coefficient to prevent internal field values of y from becoming zero or negative. It is frequently not necessary to code such a limit explicitly, for example for the heterogeneous chemical reaction, Eq. (42), the mass flux/wall velocity will automatically go to zero as the concentration/mass fraction diminishes. Similarly in an osmotic membrane, the wall velocity is not constant but rather given by,

$$U_B = L_p(\Delta p - \Delta\Pi) \tag{43}$$

where L_p is the membrane permeability, Δp is the pressure difference across the membrane and the osmotic pressure, Π, is a function of the local mass fraction, $\Pi(y_B)$, computed by means of Eq. (11).

5.3. Maxwell–Stefan equations

The CMTBC formulation, Eq. (8), is not restricted to problems where the binary or 'mixture' [42], form of Fick's law is applicable. One can still set $j_i'' = \dot{m}''\left(y_{i,T} - y_i\right)$ on $\partial\Omega$ when Fick's law does not apply within Ω; for example situations where it is required to invert the Maxwell–Stefan equation [14] to obtain the generalized Fick's law for the diffusion fluxes,

$$\mathbf{j}_i = -\sum_{i\neq j} \Gamma_{ij}\nabla y_i \text{ in } \Omega \tag{44}$$

or any other suitable constitutive closure scheme. The CMTBC is quite general. Conversely, the fixed wall value approach, above, is based on a 1-D Fick's law and the wall value must be treated consistently with Eq. (44).

5.4. Heat transfer

Heat transfer BCs may be similarly formulated by replacing y by enthalpy, h, or temperature, T. The heat added is $\dot{q}'' = \dot{m}''h_T$ [19], with

$$h_T = h_B - \frac{\dot{q}_W''}{\dot{m}''} \tag{45}$$

or $\dot{q}'' = \dot{m}''c_P T_T$ where $T_T = T_B - \dot{q}_W''/\dot{m}''c_P$, provided the Lewis number, Le = 1. The analogue of Eq. (25) is then $Fh_T = Fh_P + F\left(h_T - h_P\right)$. $\dot{q}_W''$ is external heat added, e.g., by conduction and/or radiation. Another type of heat source to consider would be reversible and irreversible entropy changes associated with heterogeneous chemical reactions at the surface of the wall.

For $\dot{m}'' = 0$, if the external heat is supplied/removed according to $\dot{q}_W'' = \alpha(T_T - T_B)$, the quantity α supplants ρU in Eq. (19), with T (or h) replacing y as the dependent variable. Therefore the results of Table 1 remain in effect; with $P = 0$, the wall value, T_B, is just the harmonic average of T_P and T_T (which in this case is the exterior or ambient temperature), i.e., $T_B = \lambda T_P + (1-\lambda)T_T$, where $\lambda = 1/(1+\alpha\delta/k)$ which is just the analog of Section 3.1, case(ii), with the internal and external 'resistances in series'.

In many combined heat and mass transfer problems, the rate of mass transfer, $\dot{m}''$, is not known, *a priori*, but is determined from a heat balance, $\dot{m}'' = \alpha B_H$, where $B_H = (h_P - h_B)/(h_B - h_T)$ or $(T_P - T_B)/(T_B - T_T)$ is the Spalding number/driving force for heat transfer. A well-known phase change example would be evaporation/condensation: The heat flux is, $\dot{q}'' = \dot{m}''h_g + \alpha_g(T_g - T_B) = \dot{m}''h_l + \alpha_l(T_l - T_B)$. The mass flux is obtained as, $\dot{m}'' = [\alpha_g(T_g - T_B) + \alpha_l(T_l - T_B)]/h_{lg}$, T_B is the interfacial temperature between the two phases and h_{lg} is latent heat. This mass flux may then be substituted as the unknown convection coefficient, F, in the corresponding species equation(s).

5.5. Momentum transfer

The boundary term is $F\left(\mathbf{U}_T - \mathbf{U}_P\right)$, where $\mathbf{U}_T$ is a 'far-field' velocity. F is proportional to the normal velocity, i.e., the BC is quadratic in nature. For a highly permeable boundary, the tangential component of the wall value, $\mathbf{U}_B$, will be non-zero in magnitude, requiring an 'external' calculation similar to that described for the conjugate heat transfer problem in Section 5.4. For low permeability boundaries, even if the tangential wall velocity is zero, normal mass transfer will still affect the shear flow. The analogy between fluid friction and heat/transfer may be exploited as follows: For mass transfer, the normalized conductance, g/g^* changes as a function of P, see Fig. 8. The normalized cell friction, τ/τ^* behaves in a similar manner, i.e., increases for suction and decreases for injection, according to Eq. (21), but substituting a 'cell Reynolds number', $R = \rho U_B\delta/\mu$ for the cell Péclet number, P. This defaults to a laminar wall boundary condition, in the limit $\dot{m}'' \to 0$. Space constraints limit discussion of this important subject.

5.6. Turbulent reacting flow

Reactive mass transfer problems are readily amenable to the method described in this paper: The boundary conditions associated with heterogeneous surface reactions, e.g., chemical catalysis, were already introduced in Section 5.1.3. Volumetric reactions result in corresponding volumetric source terms, $\dot{m}'''y_T$ (i.e., $\dot{m}_i'''$), appearing on the right side of Eq. (5). This may then be conveniently written in terms of the driving force/Spalding number as, $\dot{m}''' = \gamma B$, where γ is a 'volumetric mass transfer coefficient'. For single-phase fluids, the sum of these terms is zero, whereas for multi-phase problems, such as combustion of liquid droplets, it is non-zero.

Turbulence in fluid mechanics has been treated in a variety of manners; from 1 and 2 equation models based on the concept of a turbulent viscosity, with or without wall functions, to more complex algebraic and Reynolds stress models, large-eddy simulations and direct numerical simulations. While turbulence fundamentally changes the nature of the fluid mechanics problem, the boundary conditions as defined in Eq. (8) remain valid.

6. Conclusions

A consolidated theorem for the convective mass transfer boundary condition in the species transport equations was presented. The problem may be posed in terms of a linear boundary condition with the mixture mass flux, F, the linear coefficient and the transferred substance state, y_T, as the boundary value so that $S_P = -F$ and $S_C = Fy_T$. It was shown that the basic fluid BCs may be loosely considered to be specific instances of this general formulation. The CMTBC is coded as a Robin condition for inflow and a Neumann condition for outflow. Alternatively, if the boundary value problem is posed in terms of a wall value, provided the internal algorithm is used consistently to compute the wall value and boundary coefficient, then the boundary prescription may be coded as a Robin condition, and is identical to the CMTBC based on the T-state in the converged form. However, the wall calculation procedure is more complex.

If the numerical scheme has a diffusion cut-off limit, as is the case with the HDS, and other schemes; erroneous values can result for suction, for $P \leq -2$. Cut-off is not, however, a problem, even when a HDS is employed internally within the interior of the domain, provided the CMTBC is employed.

One scheme that was not illustrated here was the power law difference scheme (PDS), Patankar [17]. This is virtually indistinguishable from the exact/EDS for values of B, g/g^* etc., over a very wide range of P, and is therefore eminently suitable for mass transfer analysis. However it does not enjoy widespread use, and moreover suffers from the same problem as the HDS, namely that diffusion is cut-off, albeit at a very much larger magnitude, namely, for $P \leq -10$. In view of the demonstrated poor agreement between existing schemes (UDS, CDS, HDS) in terms of B vs. P, further consideration of the PDS should perhaps be considered.

A significant disadvantage of prescribing wall values instead of the CMTBC is that wall values are not constant and must be computed iteratively as a function of the local in-cell values, y_P, during the computational cycle. Moreover, wall-based schemes will introduce interpolation errors in y_B, and this is important in osmotic membranes and heterogeneous reactors where the convection flux is a function of wall concentration. These errors are readily apparent from the discrepancies in λ, from Fig. 7. For these reasons, it is suggested that the CMTBC formulation be adopted in mass transfer problems involving filtration, chemical reactions, and other applications.

It is, in general, quite simple to program the CMTBC; for codes where a wall value/gradient must be prescribed: By first setting a zero gradient condition at the default boundary patches, and then introducing an additional BC in the form of a linearized source according to Eq. (28) or (29).

Specific conclusions/recommendations to be drawn from this study then, are as follows:

- The transferred substance state provides a convenient form for the prescription of the CMTBC as a Robin (linearized) BC for inflow, and a Neumann condition for outflow.
- Conventional inlets, outlets, and walls may all be considered to be specific instances of the CMTBC.
- In low flow rate mass transfer theory, the common prescription, $\tilde{B} = \tilde{P}$, could more accurately be replaced by $\tilde{B} = \tilde{P}/(1 - \tilde{P}/2)$.
- If it is required that a wall BC must be implemented rather than the CMTBC, both the coefficient and value must be computed consistently using the same scheme. The wall values need to be updated repeatedly during the iteration cycle.
- For codes of the type shown in Fig. 3(a), the scheme used to compute the wall value must be the same as used for interior cells, however for the type shown in Fig. 3(b), this is not necessary.
- A constant B is indicative of a generic fully-developed condition, with constant value and constant flux as the two limits.

Funding

This research did not receive any specific grant from funding agencies in the public, commercial, or not-for-profit sectors.

Declaration of competing interest

The authors declare that they have no known competing financial interests or personal relationships that could have appeared to influence the work reported in this paper.

Acknowledgments

The author is indebted to Dr. N.P. Waterson who patiently read a draft of this manuscript, and made a number of constructive comments and suggestions on the contents. The author thanks Concentration Heat and Momentum (CHAM) for providing the author with the PHOENICS code.

Appendix. Comparison with Patankar approach

The book by Patankar [17] contains a detailed discussion of the finite volume method in the context of fluid flow and heat transfer, but does not dwell on mass transfer issues. It is shown below that the present work is entirely equivalent to the derivation in [17]. The amount of mass of the species of interest that is transferred by diffusion at W is

$$j = F\left(y_T - y_B\right) \tag{A.1}$$

The reader will note that this form is similar-to, but not the same as Eqs. (28) (29). Rearranging;

$$j = \frac{F}{\exp P}\left(y_T - y_P\right) = \frac{PD}{\exp P}\left(y_T - y_P\right) \tag{A.2}$$

This is the form required to prescribe the wall flux or gradient in the linear algebraic equations, Eq. (22). The reader will note that by substituting for y_B from Eq. (10), the following form [17] is obtained;

$$j = \frac{F}{\exp P - 1}\left(y_B - y_P\right) \tag{A.3}$$

However, if y_B is not known, *a priori*, Eq. (A.2) is the preferred form. In order to compare the present results with the derivation of Patankar; from Eqs. (10)–(20) it is seen that y_T is given by,

$$y_T = y_B + \frac{y_B - y_P}{\exp(P) - 1} = y_P + \frac{\exp(P)}{\exp(P) - 1}\left(y_B - y_P\right) \tag{A.4}$$

so that from Eq. (25)

$$j_{\mathrm{TOT}} = F\left(y_B + \frac{1}{\exp P - 1}\left(y_B - y_P\right)\right) = F\left(y_P + \frac{\exp P}{\exp P - 1}\left(y_B - y_P\right)\right) \tag{A.5}$$

The reader can verify that Eq. (A.5) corresponds precisely to Eq. (5.24) in the book by Patankar [17] (see also Eq. 5.26b). Comparing Eqs. (25) and (A.5)

$$F\left(y_T - y_P\right) = F\frac{\exp P}{\exp P - 1}\left(y_B - y_P\right) = a_N\left(y_N - y_P\right) \tag{A.6}$$

$$\frac{a_B}{D} = P\frac{\exp P}{\exp P - 1} = \frac{g}{g^*} + P \tag{A.7}$$

The first term, g/g^* on the right-hand side of Eq. (A.7) may be considered as the diffusive contribution to the total flux, with the second term, P, the convective component.

Since from Eq. (8) it is apparent that $j_W{}'' = \dot{m}''\left(y_T - y_B\right)$, i.e., $j_W{}'' = \dot{m}''\left(y_T - y_P\right)/\exp \mathrm{P}$ and the explicit Neumann form of the BC with $\lambda = \exp(-P)$ is recovered.

Nomenclature

English

D	Diffusivity, m^2/s
$\dot{q}''$	Heat flux, $W/(m^2\ s)$
$\dot{m}''$	Overall/mixture mass flux, $kg/(m^2\ s)$
$\dot{m}_i''$	Species i mass flux, $kg/(m^2\ s)$
$\mathbf{a}$	Matrix of coefficients
$\mathbf{b}$	Source-term vector
$\mathbf{y}$	Mass fraction vector
$\hat{\boldsymbol{n}}$	Unit outward normal
A	Area, m^2
a	Coefficient in finite-volume equations
a_i	Reaction stoichiometric coefficient
b_i	Product stoichiometric coefficient
C	Source-term coefficient in finite-volume equations
c_P	Specific heat, J/(kg K)
D	Diffusion coefficient, kg/s
F	Convection coefficient, kg/s
g	Mass transfer coefficient, $kg/(m^2\ s)$
H	Duct wall to centerline distance, m
h	Enthalpy, J/kg
j_i''	Diffusive flux of species i, $kg/(m^2\ s)$
j_i	Diffusive transport of species i, kg/s
j_{TOT}''	Total flux, $kg/(m^2\ s)$
j_{TOT}	Total transport, kg/s
k	Thermal conductivity, W/(m K)
k_i	Reaction rate, $kg/(m^2\ s)$
L_p	Hydraulic permeability, m/(Pa s)
N_B	Number of boundaries at patch
p	Pressure, Pa
S	Source term
T	Temperature, K

t	Time, s
U	Mixture velocity, m/s
U_i	Species i velocity, m/s
V	Source-term value in finite-volume equations
y, y_i	Mass fraction, kg/kg

Greek

α	Heat transfer coefficient, W/m^2 K
δ	Cell node-to-wall distance, m
ϵ	Error
Γ	Exchange coefficient, kg/(m s)
γ	Constant in blended difference schemes
γ	Volumetric mass transfer coefficient, kg/(m^3 s)
λ	Weighting function
μ	Dynamic viscosity, Pa s
ν_i	Species reaction order
ϕ	General scalar
Π	Osmotic pressure, Pa
ρ	Mixture density, kg/m^3
ρ_i	Partial density, kg/m^3
τ	Shear stress, N/m^2

Subscript

B	Boundary
g	Gas
H	Heat transfer
i	Species i
l	Liquid
N	Neighbor value
P	Nodal value
T	Transferred substance state
TOT	Total (convective+diffusive)

Non-dimensional numbers

P	Cell Péclet number, $\dot{m}''/g^*$
$\tilde{B}$	Macroscopic Spalding number, $(y - y_W)/(y_W - y_T)$
$\tilde{P}$	Macroscopic Péclet number, $Re \cdot Sc$
ξ	Normalized displacement, y/H
B	Cell Spalding number, $(y - y_B)/(y_B - y_T)$
b	Blowing parameter, $\rho U_B/g^*$
c_f	Friction coefficient, $\tau_W/\frac{1}{2}\rho U^2$
Le	Lewis number, $k/(c_P\Gamma)$
R	Cell Reynolds number, $\rho U_B\delta/\mu$
ξ	Non-dimensional distance, $\frac{1}{3}\frac{U_W}{U}\frac{x}{H}\tilde{P}^2$

Superscript

$'''$	Per unit volume
$''$	Per unit area
$'$	Per unit length
$.$	Per unit time
0	Reference state

Abbreviations

BC	Boundary condition
CDS	Central difference scheme
CFD	Computational fluid dynamics
CMTBC	Convective mass transfer boundary condition
EDS	Exponential difference scheme
HDS	Hybrid difference scheme
MUSCL	Monotonic Upstream-centered scheme for Conservation Laws
PDS	Power law difference scheme
QUICK	Quadratic-Upwind Interpolation scheme for Convective Kinematics
TVD	Total-Variation diminishing
UDS	Upwind difference scheme

Data availability

Data will be made available on request.

References

[1] P.M. Gresho, R.L. Sani, Introducing four benchmark solutions, Internat. J. Numer. Methods Fluids 11 (7) (1990) 951.
[2] D.B. Spalding, A standard formulation of the steady convective mass transfer problem, Int. J. Heat Mass Transfer 1 (1960) 192–207.
[3] S.B. Beale, Mass transfer in plane and square ducts, Int. J. Heat Mass Transfer 48 (15) (2005) 3256–3260.
[4] S.B. Beale, J.G. Pharoah, A. Kumar, Numerical study of laminar flow and mass transfer for in-line spacer-filled passages, J. Heat Transfer 135 (1) (2013) 011004.
[5] S.B. Beale, S. Zhang, M. Andersson, R.T. Nishida, J.G. Pharoah, W. Lehnert, Heat and mass transfer in fuel cells and stacks, in: A. Runchal (Ed.), 50 Years of CFD in Engineering Sciences: A Commemorative Volume in Memory of D. Brian Spalding, Springer, Singapore, 2020, pp. 485–511.
[6] K.Y. Toh, Y.Y. Liang, W.J. Lau, G.A. Fimbres Weihs, A review of CFD modelling and performance metrics for osmotic membrane processes, Membranes 10 (10) (2020).
[7] L. Chen, B. Wu, Research progress in computational fluid dynamics simulations of membrane distillation processes: A review, Membranes 11 (7) (2021).
[8] Y. Liang, D. Fletcher, Computational fluid dynamics simulation of forward osmosis (FO) membrane systems: Methodology, state of art, challenges and opportunities, Desalination 549 (2023) 116359.
[9] E.S. Oran, J.P. Boris, Numerical Simulation of Reactive Flow, second ed., Cambridge University Press, 2000.
[10] R. Probstein, Physicochemical Hydrodynamics: An Introduction, Butterworths, Boston, 1989.
[11] C. Truesdell, R. Toupin, The classical field theories, Principles of classical mechanics and field theory/Prinzipien der Klassischen Mechanik und Feldtheorie, Springer, 1960, pp. 226–858.
[12] A.E. Green, P.M. Naghdi, A dynamical theory of interacting continua, Internat. J. Engrg. Sci. 3 (2) (1965) 231–241.
[13] A.E. Green, P.M. Naghdi, A note on mixtures, Internat. J. Engrg. Sci. 6 (11) (1968) 631–635.
[14] R. Taylor, R. Krishna, Multicomponent Mass Transfer, Wiley-Interscience, New York, 1993.
[15] R. Bird, W. Stewart, E. Lightfoot, Transport Phenomena, Wiley, New York, 1960.
[16] D.B. Spalding, Convective Mass Transfer; An Introduction, Edward Arnold, London, 1963.
[17] S.V. Patankar, Numerical Heat Transfer and Fluid Flow, Hemisphere, New York, 1980.
[18] A.F. Mills, Mass Transfer, Prentice Hall, Upper Saddle River, N.J, 2001.
[19] W. Kays, M. Crawford, B. Weigand, Convective Heat and Mass Transfer, fourth ed., McGraw-Hill, New York, 2005.
[20] J.H. Ferziger, M. Perić, R.L. Street, Computational Methods for Fluid Dynamics, Springer International Publishing, 2020.
[21] A.W. Date, Introduction To Computational Fluid Dynamics, Cambridge University Press, 2005.
[22] S. Mazumder, Numerical Methods for Partial Differential Equations: Finite Difference and Finite Volume Methods, Academic Press, 2015.
[23] F. Moukalled, L. Mangani, M. Darwish, The Finite Volume Method in Computational Fluid Dynamics, Springer, 2016.
[24] S.B. Beale, M.R. Malin, H. Marschall, Remarks on the physical basis for the construction of diffusion flux terms in finite-volume equations, Comput. Therm. Sci.: Int. J. 16 (3) (2024) 71–87.
[25] H.G. Weller, G. Tabor, H. Jasak, C. Fureby, A tensorial approach to computational continuum mechanics using object-oriented techniques, Comput. Phys. 12 (6) (1998) 620–631.
[26] Concentration Heat and Momentum, PHOENICS website, 2025, URL https://www.cham.co.uk/phoenics.php.
[27] R. Courant, E. Isaacson, M. Rees, On the solution of nonlinear hyperbolic differential equations by finite differences, Comm. Pure Appl. Math. 5 (3) (1952) 243–255.
[28] D. Spalding, A novel finite-difference formulation for differential expressions involving both first and second derivatives, Internat. J. Numer. Methods Engrg. 4 (1972) 551–559.
[29] M. Perić, A Finite Volume Method for the Prediction of Three-Dimensional Fluid Flow in Complex Ducts (PhD), Imperial College, University of London, 1985.
[30] N.P. Waterson, H. Deconinck, Design principles for bounded higher-order convection schemes–a unified approach, J. Comput. Phys. 224 (1) (2007) 182–207.

[31] S.B. Beale, D.H. Schwarz, M.R. Malin, D.B. Spalding, Two-phase flow and mass transfer within the diffusion layer of a polymer electrolyte membrane fuel cell, Comput. Therm. Sci. 1 (2) (2009) 105–120.
[32] S.B. Beale, A Simple Electrochemical Cell Model, Springer, 2022, pp. 21–57.
[33] S. Zhang, S. Hess, H. Marschall, U. Reimer, S.B. Beale, W. Lehnert, openFuelCell2: A new computational tool for fuel cells, electrolyzers, and other electrochemical devices and processes, Comput. Phys. Comm. 298 (2024) 109092.
[34] T.K. Sherwood, P.L.T. Brian, R.E. Fisher, L. Dresner, Salt concentration at phase boundaries in desalination by reverse osmosis, Ind. Eng. Chem. Fundam. 4 (2) (1965) 113–118.
[35] R.M. Smith, A.G. Hutton, The numerical treatment of advection: A performance comparison of current methods, Numer. Heat Transfer Part A Appl. 5 (4) (1982) 439–461.
[36] A.K. Runchal, CONDIF: A modified central-difference scheme for convective flows, Internat. J. Numer. Methods Engrg. 24 (8) (1987) 1593–1608.
[37] B.P. Leonard, The QUICK algorithm - A uniformly third-order finite-difference method for highly convective flows, Comput. Methods Fluids (1980) 159–195.
[38] A. Harten, High resolution schemes for hyperbolic conservation laws, J. Comput. Phys. 49 (3) (1983) 357–393.
[39] B. Van Leer, Towards the ultimate conservative difference scheme. ii. Monotonicity and conservation combined in a second-order scheme, J. Comput. Phys. 14 (4) (1974) 361–370.
[40] A.S. Berman, Laminar flow in channels with porous walls, J. Appl. Phys. 24 (9) (1953) 1232–1235.
[41] J.B. Scarborough, Numerical Mathematical, Oxford and IBH Publishing, 1955.
[42] C.R. Wilke, Diffusional properties of multicomponent gases, Chem. Eng. Prog. 46 (2) (1950) 95–104.